Aerodynamic Design of a Mach 2.2 Supersonic Cruise Aircraft

R.L. Radkey,* H.R. Welge,† and R.L. Roensch‡
McDonnell Douglas Corporation, Long Beach, Calif.

The McDonnell Douglas Corporation has conducted numerous Mach 2.2 supersonic aircraft design and integration studies in support of the NASA Supersonic Cruise Aircraft Research (SCAR) program. This program traces the evolution of a baseline study configuration and an improved performance configuration through several aerodynamic design and trade study cycles. The impact of real-world constraints on configuration design is discussed. Previous studies have not addressed the Mach 2.2 cruise design condition and this work has resulted in a structurally feasible configuration capable of achieving L/D's in excess of 9 at this cruise Mach number. The purpose of this paper is to present the resulting design and wind-tunnel test results for two configurations. The wind-tunnel test results are compared to the analysis methods.

Introduction

IN 1972, interest was renewed both at NASA and in the industry in conducting technology assessment studies on supersonic cruise aircraft. The NASA Supersonic Cruise Aircraft Research (SCAR) program emerged late in 1972, charged with the task of identifying, through aircraft design studies, key technologies whose pursuit would lead to improved aerodynamic efficiency, reduced operating costs, and environmental compatibility for typical next-generation supersonic cruise configurations. McDonnell Douglas (MDC) reassessed the entire spectrum of supersonic travel beginning with a market analysis and a review of technology available at various design Mach numbers. Results of these preliminary design studies indicated that a 273-passenger, Mach 2.2 aircraft offered the best mix of low operating costs, productivity, near-term technology materials, and reduced program risk for typical supersonic transport configurations.[1] Using this as a starting point, McDonnell Douglas conducted numerous aerodynamic studies, trade studies, and sizing studies in support of the SCAR program.[2,3] A baseline study configuration, shown in Fig. 1, emerged, which was a structurally feasible arrow-wing configuration promising good cruise L/D's. Subsequent studies indicated that improved performance was available through wings optimized to reduce configuration trim drag. In 1975, a cooperative MDC-NASA wind-tunnel test program was conducted in which the performance of the study baseline configuration and an improved-performance configuration was substantiated, and the analytical techniques used in their design were validated.

Methods of Analysis

The primary analytical tools used in the aerodynamic design and analysis of the McDonnell Douglas advanced supersonic cruise aircraft configuration have been the Woodward program[4] and the Douglas Arbitrary Body Wave Drag Program.[5] The McDonnell Douglas version of the Woodward program has been extensively modified to improve its versatility. In the SCAR studies it was used in both the inverse (optimization) and direct (analysis) modes. Wings were designed by optimizing the wing camber distributions for minimum drag due to lift at specified C_L's, with and without specified pitching moments. Wings were primarily optimized as wings alone extended to the fuselage centerline, but some optimizations were done in the presence of the fuselage. Drag due to lift and wing-body pitching moments were computed by direct analysis of wing-body combinations including wing thickness effects. Wing panels were spaced equally spanwise and chordwise on both wings alone and wings exterior to the fuselage. All wings were represented by 9 spanwise and 12 chordwise panels, which is sufficient for converged solutions. Biquadratic interpolation was used to determine exterior wing camber distributions from wing-alone optimizations, and vice versa. A typical Woodward wing-body paneling scheme is shown in Fig. 2. Although not depicted on Fig. 2, the Woodward program was used in the full configuration mode to calculate wing-body pitching moments, including the effects of forebody lift.

Configuration zero-lift wave drag was calculated using the McDonnell Douglas-developed Arbitrary Body Wave Drag Program which calculates, based on the area rule theory,[6,7] the wave drag of completely arbitrary configurations. All analyses were performed on full wing-body and wing-body-nacelle configurations at their cruise attitudes. While the program can accept cambered fuselages with exact cross sections, it has been determined that cambered fuselages with

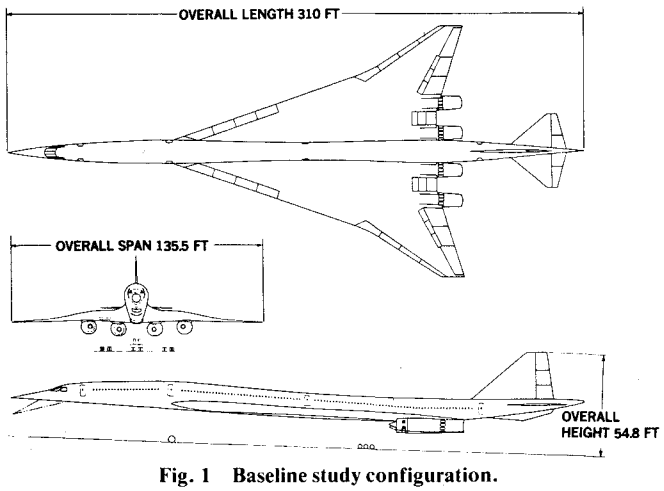

Fig. 1 Baseline study configuration.

Presented as Paper 76-955 at the AIAA Aircraft Systems and Technology Meeting, Dallas, Texas, Sept. 27-29, 1976; submitted Nov. 9, 1976; revision received Dec. 13, 1977.

Index categories: Configuration Design; Aerodynamics.

*Engineer Scientist/Specialist, Douglas Aircraft Div.
†Unit Chief, Douglas Aircraft Div. Associate Fellow AIAA.
‡Principal Staff Engineer, Douglas Aircraft Div. Member AIAA.

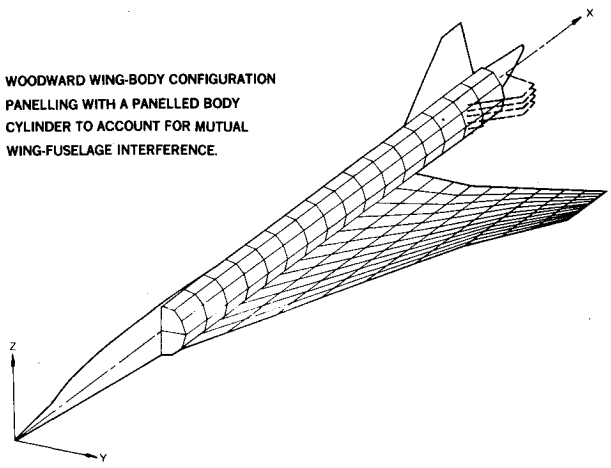

Fig. 2 Woodward Program wing-body paneling.

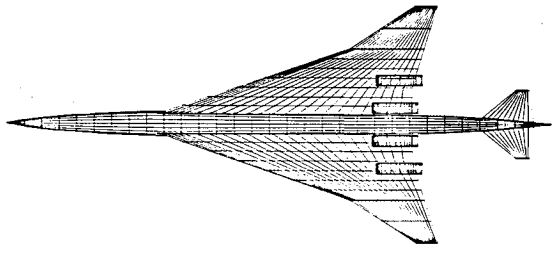

Fig. 3 Douglas Arbitrary Body Wave Drag Program paneling.

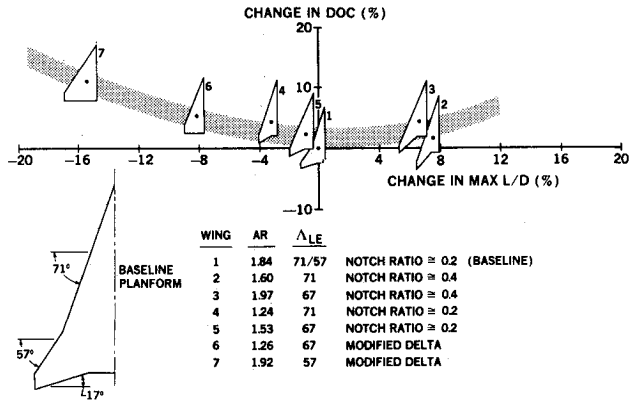

Fig. 4 Wing planform trade study.

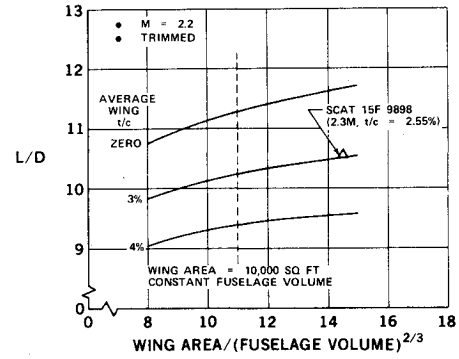

Fig. 5 Initial wing area-wing thickness study.

equivalent-area circular cross sections give the same wave drags to within 2%, so they were used exclusively during the design process. Fuselage area distributions for all configurations were optimized in the presence of wing and nacelles to give the minimum wave drag subject to minimum cross-sectional area constraints at three axial locations. These constraints were used to ensure adequate cockpit and cabin dimensions. A typical wave drag input configuration is shown in Fig. 3.

Drag polars are the sum of the Woodward drag due to lift, the arbitrary body wave drag, and the skin friction drag. Skin friction drag was computed based on adiabatic-wall smooth-flat-plate turbulent friction coefficients.[8] Skin friction drag was multiplied by two supersonic drag factors: 1.06 for roughness, suggested by NASA, and 1.05 for contingency. Based on NASA experience,[9] it was assumed that the wing would be reflexed for slender, low-cowl angle nacelles so as to prevent any additional drag in excess of the nacelle drag increment due to skin friction and installed zero lift wave drag.

Initial Studies

Wing Planform Trade Study

A wing planform trade study was conducted early in the development of the MDC Mach 2.2 baseline study configuration to establish a starting point for further studies. The baseline study planform, similar to the NASA SCAT 15F planform, had a leading-edge break at 63% semispan and leading-edge sweeps of 71 deg inboard and 57 deg outboard. The trailing edge had a planform break at 36% semispan with no sweep inboard and slightly more than 17 deg of sweep outboard. Change in Direct Operating Cost (DOC) from the baseline planform was used as the figure of merit for the study because it included consideration of structural weight and wing low-speed characteristics as well as cruise characteristics. Structural weight changes were obtained using standard McDonnell Douglas equations based on the wing geometry. As shown in Fig. 4, none of the planforms investigated had lower DOC's than the initial baseline, and it was formally adopted as the baseline configuration planform.

Wing Area and Thickness Study

A simplified study was conducted in which L/D's were calculated for a matrix of wing areas and average wing thicknesses. L/D's were plotted against a nondimensional ordinate (wing area)/(fuselage volume)$^{2/3}$ in order to allow comparison with other supersonic configurations. The results of the study, as shown in Fig. 5, were used initially to size the baseline configuration. A wing area of 10,000 ft^2 and an average wing thickness to chord ratio (t/c) of 3% were selected for the baseline in order to meet a 4000-n.mi. range requirement at 750,000 lb takeoff gross weight with a reasonable takeoff field length. The study indicated that for a wing area of 10,000 ft^2 and a constant fuselage volume (the dashed vertical line on Fig. 5), a maximum possible L/D of about 11.3 could be achieved in the limit of a zero-thickness wing properly optimized for minimum drag due to lift.

Advanced Studies—Baseline Configuration

Planform Modifications

Numerous planform modifications intended to improve the configuration's low- and high-speed performance were examined. A series of wings having the same leading-edge sweeps as the baseline but with aspect ratios increased from the baseline 1.84 up to 2.0 were found to have reduced drag due to lift. However, the structural weight increases for these planforms were found to be more than offsetting, and a net reduction in range resulted for each of the sized configurations. Consequently, the baseline planform was retained for the remainder of the studies.

Baseline Wing Camber Optimization

The baseline wing camber surface was originally conceived as a straightforward Woodward optimization of the camber

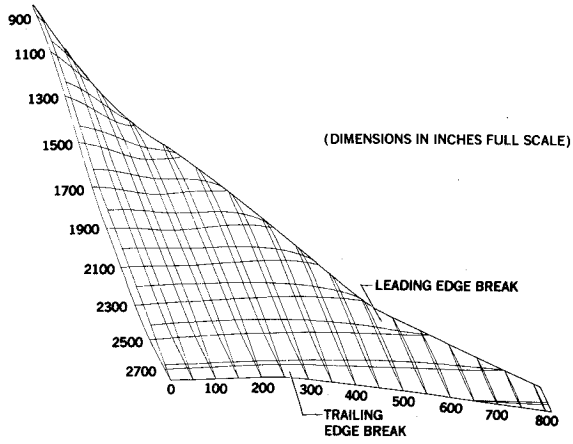

Fig. 6 Baseline wing camber and thickness.

distribution for minimum drag due to lift at the cruise C_L. The resulting output camber slopes integrated to a camber surface having about 6 deg of incidence near the wing-fuselage intersection. Current thinking held that the optimum wing-fuselage combination should have the fuselage positioned along the wing centerline camber line with the nose and tail aligned with the freestream.[9] However, various constraints on the layout of the configuration required that the wing be modified to have an incidence of 4 deg near the wing-fuselage intersection. This was accomplished by rotating the inboard defining wing section nosedown from 6 to 4 deg.

The Woodward program has a dihedral capability, but optimizations are planar and the spanwise vertical positioning of wing sections, or shear distribution, is arbitrary. A shear distribution for the baseline wing was selected by choosing a wing trailing-edge vertical height spanwise distribution which improved engine ground clearance slightly. The final sheared baseline wing is shown in Fig. 6. The small amount of vertical shear did not affect the aircraft lateral stability.

Wing Thickness Distribution Studies

Selection of the wing thickness distribution required an integrated effort by Aerodynamics and Structures. Studies were conducted to determine the zero-lift wave drag and structural weight of various thickness arrangements. The weights were based on optimizing the size of the structural elements for wing twist, deflection, roll effectiveness, and aerodynamic center shift. In addition, for selected configurations, a reoptimization for flutter was performed. The allowables for structural materials were reduced to account for high temperature, thermal gradients, and fail-safety.

Thickness distibutions for the baseline wing were specified by defining section thickness distributions at the spanwise locations of the wing root, the trailing-edge planform break, the leading-edge planform break, and the tip, and using straight-line development between the sections. For the three wing panels defined by the planform breaks, the two inboard panels had a modified 66-00X thickness section and the outboard panel had a biconvex thickness section.

Specification of the thickness distribution on the two inboard wing panels was constrained by a need for sufficient internal volume to stow the landing gear and a need for sufficient rear spar depth to adequately limit wing aeroelastic deflections. A study was conducted to determine the thickness distribution which would yield the best combination of low drag and low weight. Wave drag and structural weight were calculated for the matrix of arrangements shown in Fig. 7, and the lowest total equivalent weight arrangement was identified.

The effects of structural constraints and wave drag variation are shown in Fig. 8 in terms of idealized structural wing box weight. Clearly, as the outboard panel thickness increases, the drag equivalent weight increases and the structural weight decreases. Figure 8 illustrates this relationship for outboard panels having the same t/c at the leading-edge break and wing tip. The analysis, however, included the effects of the independent variation of maximum t/c at the leading-edge break and at the tip.

The variation in aircraft range due to various outboard panel thickness arrangements was calculated for a fixed takeoff gross weight, engine size, and payload. The results of the study indicated that maximum range was obtained with maximum t/c's of 2.5% at the leading-edge break and 3.5% at the tip. The maximum range curves were, however, quite flat and the final outer panel maximum t/c's were selected to be 3.0% at the leading-edge break and at the tip in order to provide more space for flap and spoiler actuators. This

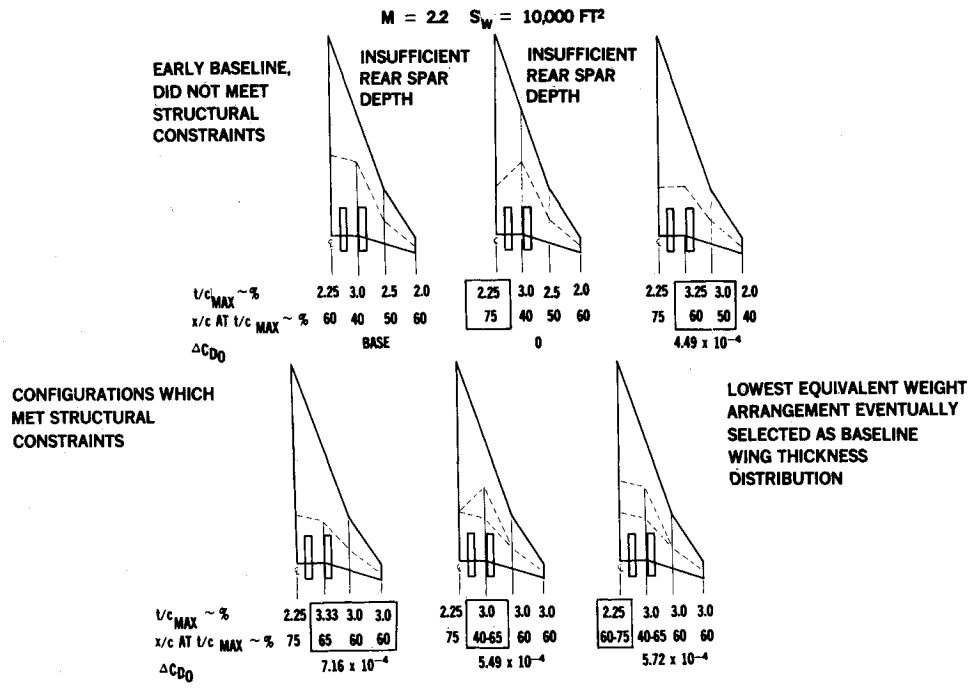

Fig. 7 Inboard panel thickness distribution study.

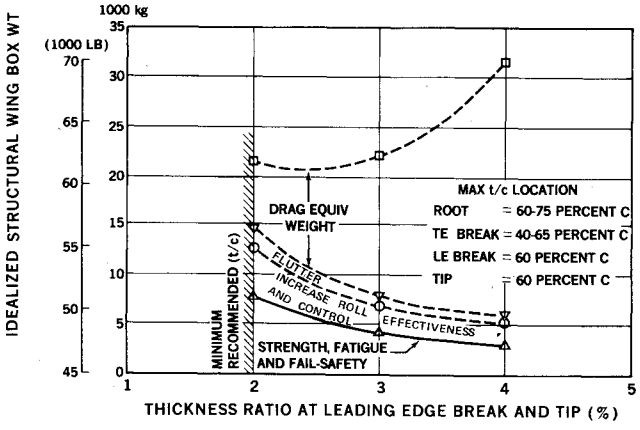

Fig. 8 Outboard panel aerostructural study.

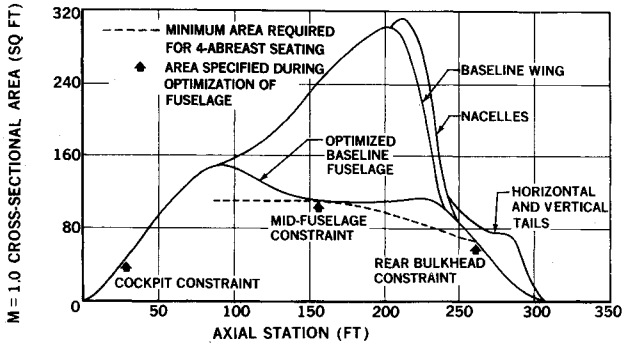

Fig. 9 $M=1.0$ cross-sectional area distribution for the baseline configuration.

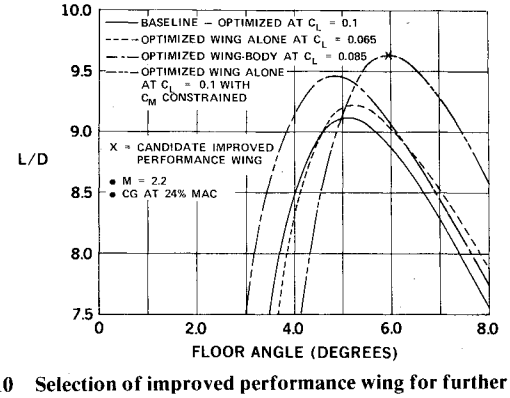

Fig. 10 Selection of improved performance wing for further study.

deviation from the optimum arrangement resulted in a range penalty of about 20 n.mi.

Nacelles

The baseline configuration nacelle arrangement consisted of a set of four axisymmetric cambered nacelles located beneath the wing near the wing trailing edge. The individual pod axisymmetric nacelles were found to have the lowest installed wave drag of any of the numerous propulsion system arrangements studied. A comprehensive nacelle location study using the baseline wing resulted in the nacelles being located as shown in Fig. 1. A detailed description of the nacelle location and design process is contained in Ref. 10.

Optimizaiton of the Fuselage Area Distribution

With the wing camber, wing thickness, and nacelles specified for the baseline configuration, it was possible to refine the baseline fuselage. The fuselage camber distribution was selected to meet layout constraints on cockpit visibility, tail clearance for rotation, and placement of wing structure carry-through members. The fuselage area distribution, shown in Fig. 9, was optimized for minimum zero-lift wave drag at $M=2.2$ using the Douglas Arbitrary Body Wave Drag Program. The optimization was carried out with the fuselage cross-sectional area constrained to specified values at three fuselage stations to ensure adequate cabin volume. As indicated in Fig. 9, constraints were imposed at the cockpit station, at the fuselage midlength station, and at the rear bulkhead station. The optimization was done with nacelles installed.

Advanced Studies— Improved Performance Configuration

A series of configuration and wing camber optimization studies was conducted to see if the cruise floor angle could be reduced without penalty in L/D.[11] One of these studies was a wing optimization study in which wings were optimized at the design C_L with pitching moment constraints designed to reduce the cruise trim drag. It was observed that the baseline configuration operated with a tail download when trimmed at cruise due to a negative wing-body pitching moment. The study wings were constrained to produce more positive wing-alone pitching moments, which translated into more positive wing-body pitching moments once the wings were properly integrated with the baseline fuselage. The more positive the wing-body pitching moments at cruise, the greater the tail upload and greater the improvement in L/D. This trend continues until the camber distributions of the wings become radical enough that the penalties in drag due to lift offset the gains in trim drag. The optimum of this locus of wing designs was found to increase L/D by 0.6, but also to increase the cruise floor angle by 1.0 deg, as shown in Fig. 10.

These studies indicated that it may not be possible to both improve the aircraft cruise L/D and substantially reduce the cruise floor angle below the 5 deg of the baseline configuration solely through wing design. The cruise floor angle vs L/D trade is, however, largely academic in light of the overwhelming impact of L/D on aircraft DOC, and the studies really served to identify sources of configuration L/D improvement. As a result, the best of the constrained pitching moment optimized wings was selected for further study as an improved performance configuration.

Wind-Tunnel Test

A cooperative McDonnell Douglas-NASA wind-tunnel test[12] of the baseline and improved performance configurations was conducted at the NASA Ames facility. The test was funded as a part of the SCAR program. The test was run in the NASA Ames Unitary Plan Wind Tunnel, with Mach numbers from 0.5 to 1.3 run in the Ames 11-ft tunnel and Mach numbers from 1.6 to 2.4 run in the Ames 9-ft by 7-ft tunnel. The model was scaled at 1.5% based on a full-scale wing area of 10,000 ft^2. All data were taken at a unit Reynolds number of 4.0×10^6 per ft which gave a model Reynolds number of 3.9×10^6 based on the wing trapezoidal mean aerodynamic chord (MAC) of 0.973 ft. This is roughly 3.5% of the full-scale flight Reynolds number at Mach 2.2. A picture of the model in the Ames 9-ft by 7-ft tunnel is presented in Fig. 11.

The purpose of this test was to explore numerous technology problems associated with the design and analysis of supersonic cruise aircraft and to create a Mach 2.2 design information data base. The test addressed the validity of design and analysis methods as applied to arrow-wing configurations. Problems of wing reflexing to achieve beneficial wing-nacelle interference and the possibility of using an external compression inlet rather than a mixed compression inlet at Mach 2.2 were also addressed but are considered in another paper.[10]

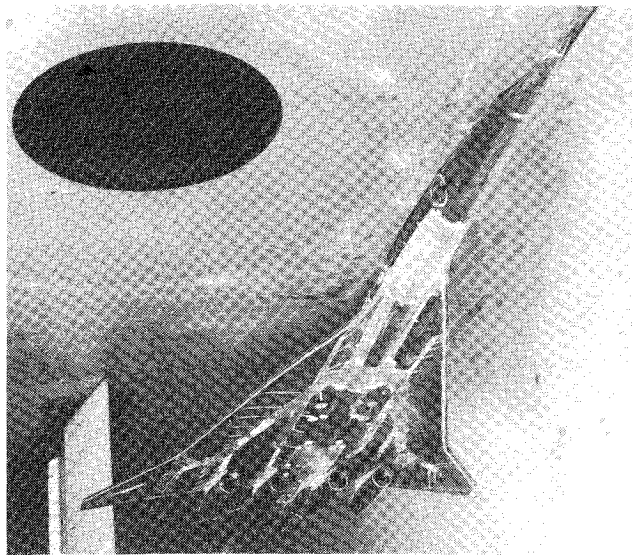

Fig. 11 High-speed model in NASA Ames 9- by 7-ft tunnel.

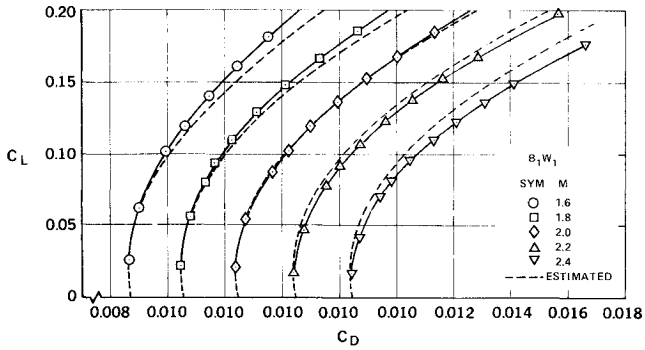

Fig. 12 Drag polars for $B_1 W_1$.

Configuration longitudinal and lateral directional aerodynamic characteristics were determined and surface pressures (247 ports) were taken simultaneously with the force data. Tuft and Schlieren pictures were also taken.

The following designations were used for the test:

- B_1 = baseline model fuselage (the aft end of the model fuselage was distorted from just aft of the wing trailing edge to accommodate the model support sting)
- W_1 = baseline wing (optimized wing alone at a C_L of 0.1)
- W_2 = improved performance wing (optimized wing alone at a C_L of 0.1 with a pitching-moment constraint designed to improve trimmed operation).

The test data have been corrected, using analytical methods, to flight conditions for the aircraft configuration with a closed afterbody. Corrections were made for the changes in skin friction drag, wave drag, and drag due to lift. Glass bead transition strips were used to fix transition on the model. The results of a transition strip drag study showed that there was no excess drag for the bead size used. Trim drag analysis has been made with analytically derived tail characteristics used in a linearized trim drag program in order to place experimental trimmed results on a consistent basis with estimated trimmed results and design analyses. This has the effect of making the trimmed results reflect only the differences between wing-body data and wing-body estimates, which is justified in light of the validation of design methods which are primarily wing-body oriented.

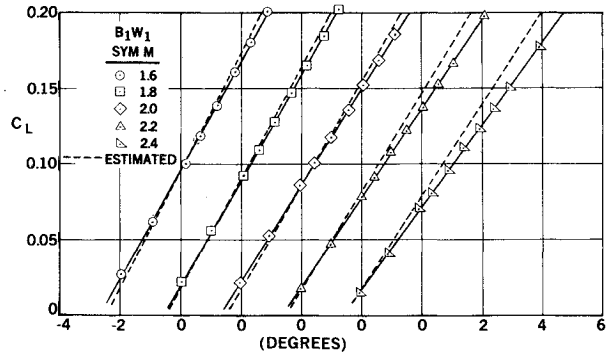

Fig. 13 Lift curves for $B_1 W_1$.

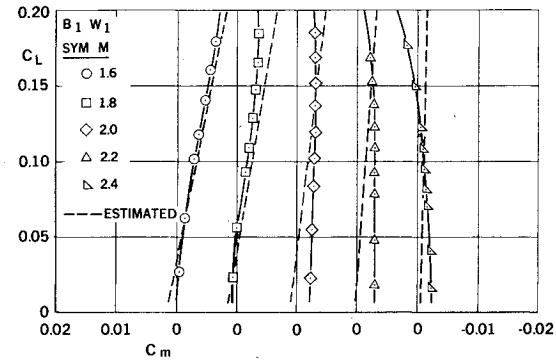

Fig. 14 C_m vs C_L curves for $B_1 W_1$.

Test Results

Basic longitudinal aerodynamic coefficients for wing-body configuration $B_1 W_1$ are shown in Figs. 12-14 for Mach numbers 1.6 to 2.4. Agreement with analytical predictions is reasonably good and the other configurations tested showed similar agreement.

The drag polars are shown in Fig. 12. Excellent agreement is shown between estimated and experimental lift independent drags. The calculated drag due to lift, however, shows a trend of overprediction at the lower supersonic Mach numbers and underprediction at the higher Mach numbers. Agreement at Mach 2.0, $0.2M$ less than the design Mach number, is excellent.

The lift curves are shown in Fig. 13. Agreement with the calculated lift curves is quite good. The experimental lift curve slopes are slightly less than predicted, and the lift is somewhat overpredicted at the higher Mach numbers. This is possibly due to the decambering effect of the boundary layer.

The pitching moment characteristics are shown in Fig. 14. Agreement is reasonably good considering the difficulty of predicting pitching moments for cambered three-dimensional configurations. Near the cruise C_L where the data are almost linear, experiment and theory are in reasonable agreement. Supersonically, all configurations show a gradual pitchup beginning well above the cruise C_L at all Mach numbers. The pitchup is not considered to be a significant problem because the horizontal tail has sufficient control authority to compensate for the change from linear pitching moments using only a small percentage of available tail effectiveness even at the design load factor.

Estimated and experimental upper surface pressures on wing W_2 at two angles of attack are shown in Fig. 15. At $\alpha = 2.46$ deg, which is near the nominal W_2 cruise angle of attack, agreement is fairly good everywhere. At the higher angle of attack, the Woodward linear theory pressures on the wing outboard panel exceed vacuum C_p's, and agreement is poor elsewhere due to strongly nonlinear upper surface flows. Similar results are observed for W_1.

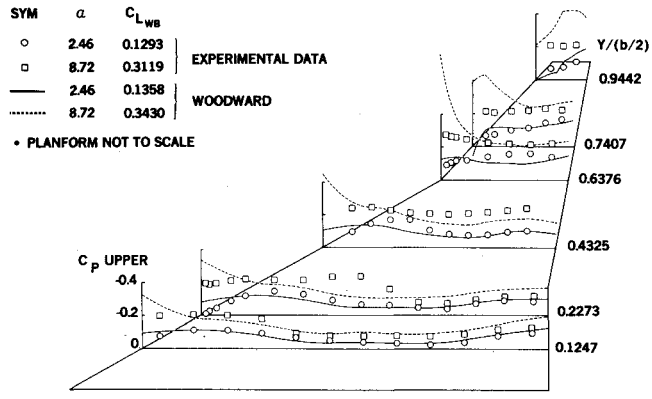

Fig. 15 Calculated and experimental upper surface pressure distributions on B_1W_2 at $M=2.2$.

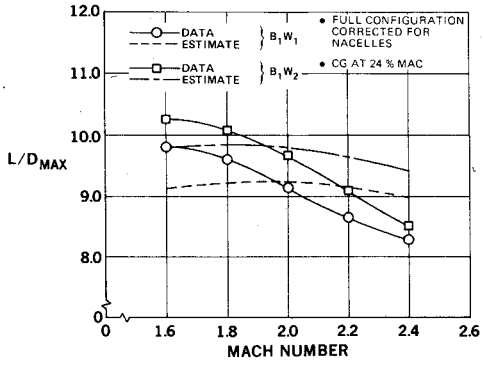

Fig. 16 Estimated and experimental trimmed $L/D_{max.}$ for B_1W_1 and B_1W_2.

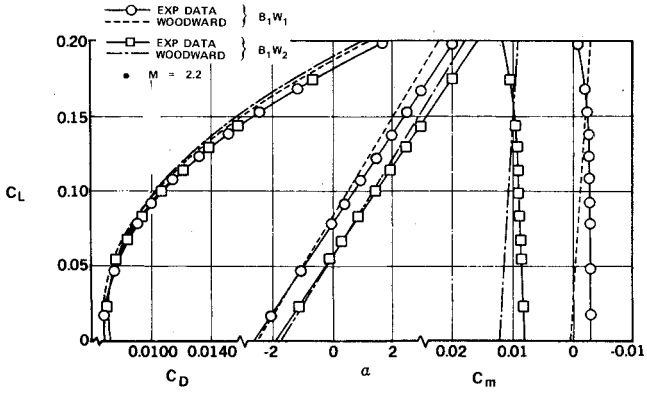

Fig. 17 Wing-body characteristics for B_1W_1 and B_1W_2 at $M=2.2$.

Curves of estimated and experimental trimmed $L/D_{max.}$ for the supersonic Mach numbers are shown in Fig. 16 for the complete configuration B_1W_1 and B_1W_2 including mixed compression nacelle/wing reflexing increments as inferred from the test data. The nacelle external skin friction drag is included in the installed engine performance and not included in the aircraft drag. The disagreement between theory and data is due to the inaccurate prediction of drag due to lift shown in Fig. 12.

Validation of Design Techniques

The evaluation of design techniques starts with an examination at Mach 2.2 of the wing-body characteristics of the baseline and improved performance wings. As shown in Fig. 17, the incremental differences in all the coefficients are exceptionally accurate. The change in C_{m_0} observed between W_1 and W_2 is of special interest because the W_2 design was

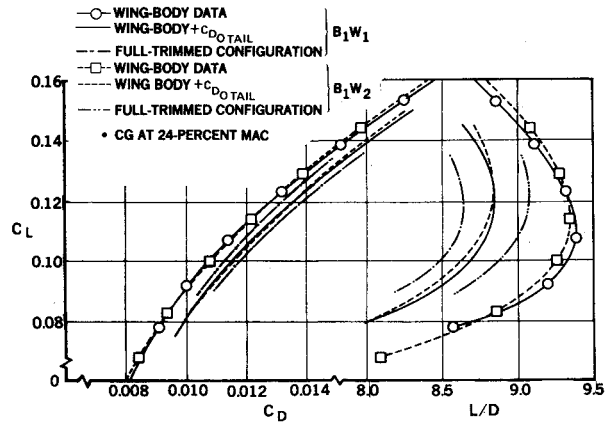

Fig. 18 Trimmed polars and L/D for B_1W_1 and B_1W_2 at $M=2.2$.

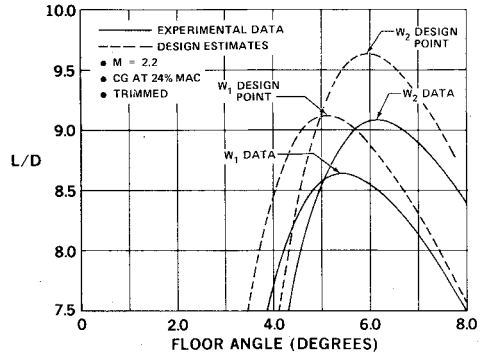

Fig. 19 L/D vs cabin floor angle for B_1W_1 and B_1W_2.

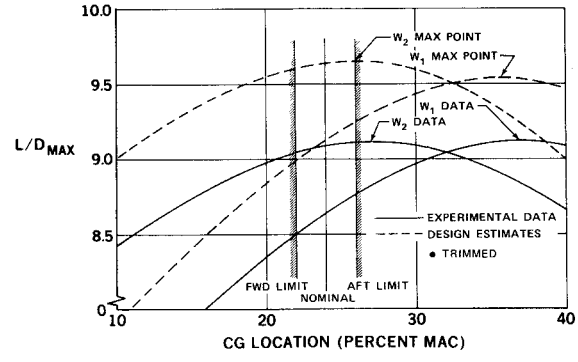

Fig. 20 $L/D_{max.}$ vs c.g. location for B_1W_1 and B_1W_2 at $M=2.2$.

predicated on making the wing-body pitching moments positive, requiring a tail upload to trim the aircraft.

For the remaining discussion, the wing-body data have been adjusted to full scale, including the increment for mixed compression nacelles without external skin friction drag.

The effect of the change in C_{m_0} on the trimmed performance of the aircraft is shown in Fig. 18. The addition of the wave drag and skin friction drag of the horizontal and vertical tails brings the untrimmed $L/D_{max.}$ down from 9.4 to 8.8 for both configurations. The tail download required to trim B_1W_1 reduces $L/D_{max.}$ to 8.64 for the baseline configuration, but the tail upload required to trim B_1W_2 raises $L/D_{max.}$ up to 9.1 for the improved performance configuration.

Recalling the studies which led to the development of W_2, a comparison of L/D versus cabin floor angle for B_1W_1 and B_1W_2 is shown in Fig. 19. The experimental L/D's are about 0.5 in L/D less than predicted due to the slightly worse than predicted drag due to lift. However, the experimental in-

crements in L/D and cabin floor angle are remarkably close to those predicted in the design process.

The variation of $L/D_{max.}$ with c.g. location is shown in Fig. 20 for B_1W_1 and B_1W_2. Again, while the level of experimental $L/D_{max.}$ is less than predicted, the experimental increments between W_1 and W_2 are almost as predicted. This figure also points out the real benefit of optimizing the wing for a desired pitching moment, that the greatest achievable $L/D_{max.}$ can be obtained within desired c.g. limits. The c.g. limits shown on Fig. 20 were chosen so that the aft supersonic limit corresponds to the subsonic neutral point.

Conclusions

Numerous technology assessment studies have been conducted in support of the NASA Supersonic Cruise Aircraft Research (SCAR) program. Combined aerodynamic-structural trade studies have been conducted leading to a structurally feasible baseline aircraft with good supersonic cruise efficiency. Compromises in aerodynamic cruise efficiency have been made to favor structural efficiency resulting in maximum aircraft range. Detailed aerodynamic design studies have been conducted making imaginative use of existing analysis and design tools, in particular the Woodward program and the Douglas Arbitrary Body Wave Drag Program, to develop an improved performance configuration. The results of a wind-tunnel test of the baseline and improved performance configurations have supported the analysis and design methods with the possible exception of some discrepancies in the prediction of drag due to lift. However, even with discrepancies in the predicted level of drag due to lift, the increments between configurations are accurate and can be used to identify further improvements in performance. The results have also verified the good aerodynamic efficiency of the configurations with a demonstrated trimmed $L/D_{max.}$ of 9.1 for the improved performance configuration. There is demonstrable evidence that further refinements are possible to raise the $L/D_{max.}$ to 9.6 and a goal of 10.3 has been set for technology research as a realistic target for the present arrow-wing-type design at Mach 2.2.

Acknowledgment

This work was partially supported by NASA Langley under Contract numbers NAS1-13633 and NAS1-13612.

References

[1] FitzSimmons, R.D. and Hoover, W.C., "AST-A Fifth Engine for Environmental Consideration," Society of Automotive Engineers, SAE Paper 730899, 1973.

[2] "Studies of the Impact of Advanced Technologies Applied to Supersonic Transport Aircraft," prepared by the Douglas Aircraft Co., under NASA contract NA51-11939, Douglas Rept. MDC J4394, 1973.

[3] FitzSimmons, R.D. and Roensch, R.L., "Advanced Supersonic Transport," Society of Automotive Engineers, SAE Paper 750617, 1975.

[4] Woodward, F.A., Tinoco, E.N., and Larsen, J.W., "Analysis and Design of Supersonic Wing-Body Combinations, Including Flow Properties in the Near Field," NASA CR-73016, 1967.

[5] Gentry, A.E., Smyth, D.N., and Oliver, W.R., "The Mark IV Supersonic-Hypersonic Arbitrary-Body Program," Air Force Flight Dynamics Laboratory, AFFDL-TR-73-159, 1973.

[6] Jones, R.T., "Theory of Wing-Body Drag at Supersonic Speeds," NACA RM A53H18a, 1953.

[7] Whitcomb, R.T., "A Study of the Zero-Lift Drag Rise Characteristics of Wing-Body Combinations Near the Speed of Sound," NACA RM L52H08, 1952.

[8] Clutter, D.W., "Charts for Determining Skin Friction Coefficients on Smooth and on Rough Flat Plates at Mach Numbers Up to 5.0 With and Without Heat Transfer," Douglas Rept. ES 29074, 1959.

[9] Baals, D.D., Robins, A.W., and Harris, R.V. Jr., "Aerodynamic Design Integration of Supersonic Aircraft," AIAA Paper 68-1018,5th Annual Meeting, Philadelphia, Pa., 1968.

[10] Welge, H.R., Radkey, R.L., and Henne, P.A., "Nacelle Aerodynamic Design and Integration Study on a Mach 2.2 Supersonic Cruise Aircraft," AIAA Paper 76-757, AIAA/SAE 12th Propulsion Conference, Palo Alto, Calif., 1976.

[11] Radkey, R.L., "An Analysis of the Impact of Cabin Floor Angle Restrictions on L/D for a Typical Supersonic Transport," NASA CR-132508, 1974.

[12] Radkey, R.L., Welge, H.R., and Felix, J.E., "Aerodynamic Characteristics of a Mach 2.2 Advanced Supersonic Cruise Aircraft Configuration at Mach Numbers from 0.5 to 2.4," NASA CR 145094, 1977.